



## Structure-properties of super-tough PLA alloy with excellent heat resistance

Kazuhiro Hashima, Shotaro Nishitsuji\*, Takashi Inoue

Department of Polymer Science and Engineering, Yamagata University, Yonezawa 992-8510, Japan

### ARTICLE INFO

#### Article history:

Received 10 March 2010

Received in revised form

3 June 2010

Accepted 24 June 2010

Available online 1 July 2010

#### Keywords:

Poly(lactic acid)

Rubber-toughening

Negative pressure

### ABSTRACT

Poly(lactic acid) (PLA) was toughed by blending hydrogenated styrene-butadiene-styrene block copolymer (SEBS) with the aid of reactive compatibilizer, poly(ethylene-co-glycidyl methacrylate) (EGMA). The high temperature property and thermal aging resistance were improved by further incorporating polycarbonate (PC), the ductile polymer with high glass transition temperature. On the basis of transmission electron microscopy, differential scanning calorimetry, and dynamic mechanical analysis, the outstanding toughness and aging resistance of the 4 component alloy; e.g., PLA/PC/SEBS/EGMA = 40/40/5/5 (wt. ratio), seems to come from the negative pressure effect of SEBS that dilates the plastic matrix consisting of PLA and PC to enhance the local segment motions.

© 2010 Elsevier Ltd. All rights reserved.

### 1. Introduction

Poly(lactic acid) (PLA) is a biodegradable polymer derived from renewable sources. Most of studies of PLA and the blends have been focused on the biodegradable [1–4] and biocompatible aspects [5–8]. PLA has a lot of drawbacks on the properties and processability; poor impact strength (a few kJ/m<sup>2</sup>), small elongation at break (a few%), low heat deflection temperature (HDT) (<60 °C), and poor processability (high temperature mold is required for the crystallization to result in long cycle time for injection molding). In literature, there are several papers to improve the mechanical properties [9–16]. All papers deal with the blending with another biodegradable polymer, such as poly( $\epsilon$ -caprolactone) and poly(butylenes succinate-co-L-lactide). The tensile and impact properties have been improved somewhat; but not enough as the engineering plastics.

The design of biodegradable polymer materials is an interesting subject. On the other hand, PLA should be interested as a green polymer from renewable sources. Then, it should be used as commodity plastics in near future. For such scenario, one should overcome the drawbacks of PLA mentioned above. Recently, we successfully developed a super-ductile poly(butylenes terephthalate) (PBT) alloy with excellent heat resistance by blending with hydrogenated styrene-butadiene-styrene block copolymer (SEBS) and a small amount of poly(ethylene-co-glycidyl methacrylate) as the reactive compatibilizer [17]. Following this blend

recipe for the analogous polyester, in this article, we tried to develop a tough PLA alloy. However, the recipe did not work well. By incorporating polycarbonate (PC) as the 4th component, a tough PLA alloy with excellent heat resistance was explored. The structure-properties relationship is discussed on the basis of transmission electron microscopy, differential scanning calorimetry and dynamic mechanical analysis.

### 2. Experimental

All raw materials in this study are commercially available polymers. Two PLAs were provided by NatureWorks Co. Ltd.: one is 3001D, injection molding grade with low viscosity (coded as PLA-l in this paper), and the other is 4032D, film extrusion grade with high viscosity (coded as PLA-h). SEBS was from Kuraray Co. Ltd.: Septon 8006, styrene content = 34 wt.%. EGMA with GMA content of 6 wt.% (Bondfast 2C) was obtained from Sumitomo Chemical Co. Ltd. PC was from Idemitsu Co. Ltd.: Taflon A1900. The polymer pellets were dried in a vacuum oven at 80 °C for at least 8 h before melt blending. Melt blending was carried out using a twin-screw extruder TEM-35BS (Toshiba Machine Co. Ltd.) with screw diameter  $D = 37$  mm and  $L/D = 31.9$ , where  $L$  is the screw length. Screw speed was set at 150 rpm. The barrel temperature was at 200 °C for binary and ternary systems (PLA/SEBS and PLA/SEBS/EGMA) and at 240 °C for PLA/PC/SEBS/EGMA system. The extruded strands were cooled in a water bath, pelletized, and dried in vacuum at 80 °C for 10 h. Injection molding was carried out by an injection machine (NP7 Real Mini, Nissei Co. Ltd.) to obtain the dumbbell specimen having stripe part of 2 mm thickness and 4 mm width (JIS-SA type) for tensile test and the bar specimen of 4 mm thick 10 mm width 80

\* Corresponding author.

E-mail address: [nishitsuji@yz.yamagata-u.ac.jp](mailto:nishitsuji@yz.yamagata-u.ac.jp) (S. Nishitsuji).

**Table 1**  
Composition (wt.%) and mechanical properties of neat PLA, binary blend, and ternary blend.

Sample code	I	II	III
PLA-I	100	70	70
SEBS	–	30	20
EGMA	–	–	10
Elongation at break, Eb (%)			
as-mold	3	178	185
aged <sup>a</sup>	3	98	100
Izod impact strength (kJ/m <sup>2</sup> )			
as-mold	3	16	92
aged <sup>a</sup>	3	7	32

<sup>a</sup> Annealed at 80 °C for 48 h.

mm length for Izod impact test and HDT measurement. The barrel temperature was set at 240 °C.

The uniaxial tensile test was carried out at room temperature using a tensile tester AG-100kNG (Shimadzu Co. Ltd.) at a crosshead speed of 5 mm/min.

Izod impact test was by an impact tester, DG-1B (Toyo Seiki Co. Ltd.) after notching (V notch: 2 mm depth/tip diameter 0.25 mm). Tensile and impact tests were carried out both for the as-mold samples and the aged samples after annealing at 80 °C for 48 h in a geer-type oven.

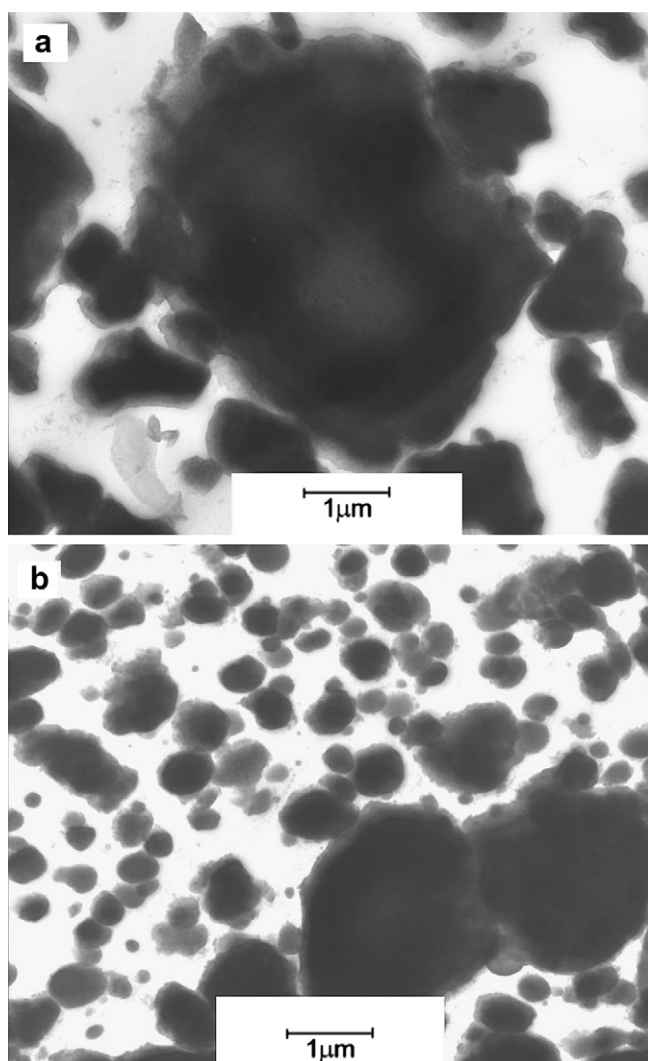


**Fig. 1.** TEM micrographs of (a) PLA/SEBS = 70/30 and (b) PLA/SEBS/EGMA = 70/20/10.

**Table 2**  
Compositions (wt.%) of 4 component systems.

Sample code	IV	V	VI	VII	VIII
PLA-I	60	50	40	–	–
PLA-h	–	–	–	60	40
PC	20	30	40	20	40
SEBS	15	15	15	15	15
EGMA	5	5	5	5	5

HDT was estimated by an HDT tester, 6M-2 (Toyo Seiki Co. Ltd.) at flat-wise mode under a load of 0.45 MPa at a heating rate of 120 K/h. HDT was the temperature at which the specimen distortion increased to 0.34 mm during the heating process.

Differential scanning calorimetry (DSC) was carried out under nitrogen flow at a heating rate of 20 K/min using Perkin–Elmer DSC-7. A tiny sample (ca. 10 mg) for DSC was picked up from a core part of the injection-molded dumbbell specimen.

Dynamic mechanical analysis (DMA) was by DMA-50N (Metravib Co. Ltd.) in a tensile mode. The dynamic loss ( $\tan \delta$ ) was measured at a frequency of 1 Hz and a heating rate of 20 K/min as a function of temperature from –150 °C to +180 °C.

Morphology was observed under a transmission electron microscopy (TEM CM300, Philips) operating at an acceleration

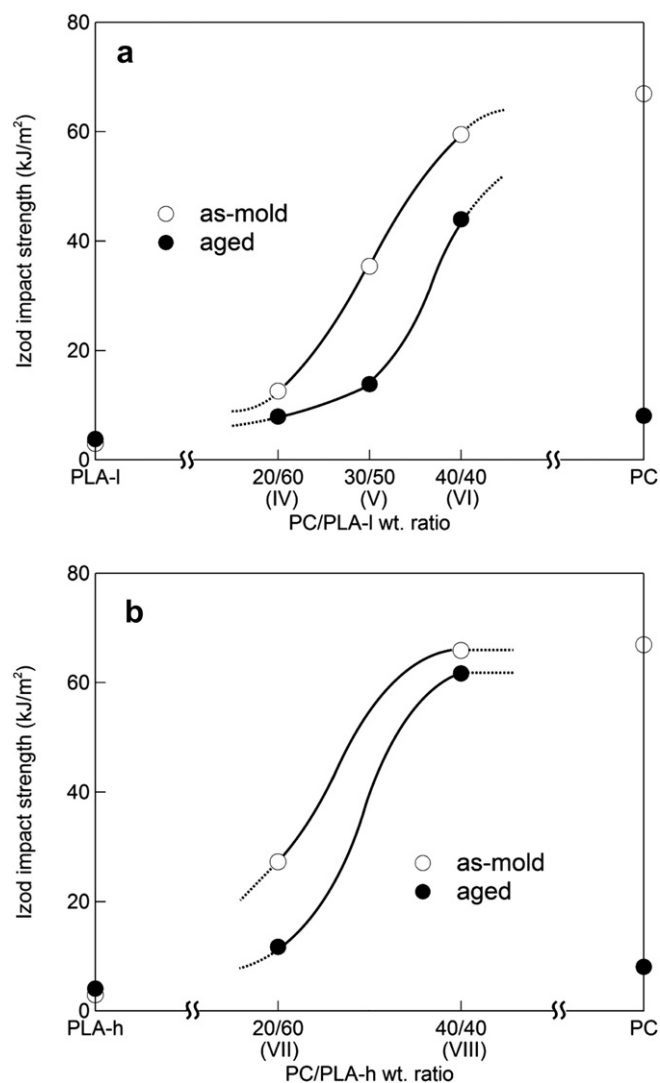


**Fig. 2.** Izod impact strength as a function of PC/PLA wt. ratio; compared with neat PLA and PC. (a) PLA-I systems, (b) PLA-h systems.

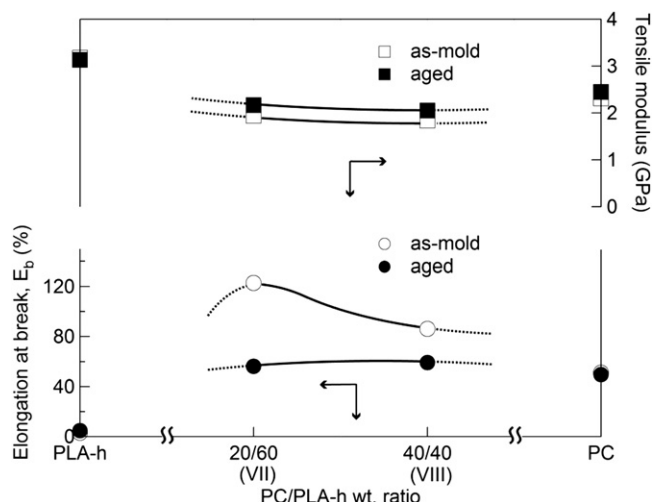


Fig. 3. Tensile properties as a function of PC/PLA wt. ratio; compared with neat PLA and PC.

voltage of 200 kV. In prior to the TEM observation, the sample picked up from the core part of molded dumbbell specimen was microtomed at  $-120\text{ }^{\circ}\text{C}$  to an ultra thin section of 70 nm thick, and then stained by ruthenium tetroxide ( $\text{RuO}_4$ ) in the gas phase at room temperature for 10 min.

### 3. Results and discussion

Table 1 shows the compositions of binary (PLA/SEBS) and ternary (PLA/SEBS/EGMA) blends and the mechanical properties of the as-mold and aged specimens, as compared with neat PLA. By adding SEBS, both the elongation at break ( $E_b$ ) and Izod impact strength are improved (sample II). However, by annealing at  $80\text{ }^{\circ}\text{C}$  for 48 h, both the tensile and impact properties are seriously damaged. By further incorporating EGMA (sample III), the Izod impact strength of as-mold specimen increases very much; however, it decreases dramatically by the annealing.

Fig. 1 shows TEM micrographs of samples II and III. Dark regions are assigned to the SEBS particles in which the characteristic domain structure of the block copolymer is seen (not so clear in Fig. 1 but obvious in Fig. 9). Average particle size in the ternary

system is much smaller than the binary system. It suggests the effect of EGMA as the reactive compatibilizer. The epoxide group of EGMA is expected to react with the chain end groups of PLA, carboxylic acid and hydroxyl groups, to yield the *in situ*-formed PLA-EGMA graft copolymer. The copolymer should play a role of emulsifier for the interface between PLA and SEBS phases to reduce the size of SEBS particles. The size reduction seems to be effective for the toughening. However, the effect is not sufficient for the aged system. By the annealing, the PLA matrix of the ternary system would become very brittle by the crystallization, and then the reduced size of rubber particle may be not small enough for the toughening [18]. Actually, DSC exothermic peak area around  $170\text{ }^{\circ}\text{C}$  (the melting point of PLA) of the as-mold ternary system was  $1\text{ J/g-PLA}$  and it increased to  $38\text{ J/g-PLA}$  after the annealing.

Anyhow, the high toughness of as-mold specimen was not retained in the aged one. To achieve the high retention, we chose a ductile polymer PC and incorporated it together with SEBS and EGMA. PC has high glass transition temperature ( $T_g = 140\text{ }^{\circ}\text{C}$ ) so that HDT is expected to be elevated by adding PC.

Compositions of the 4 component systems are shown in Table 2. Contents of SEBS and EGMA are fixed at 15 and 5 wt.%, respectively. PC content is varied from 20 to 40 wt.%.

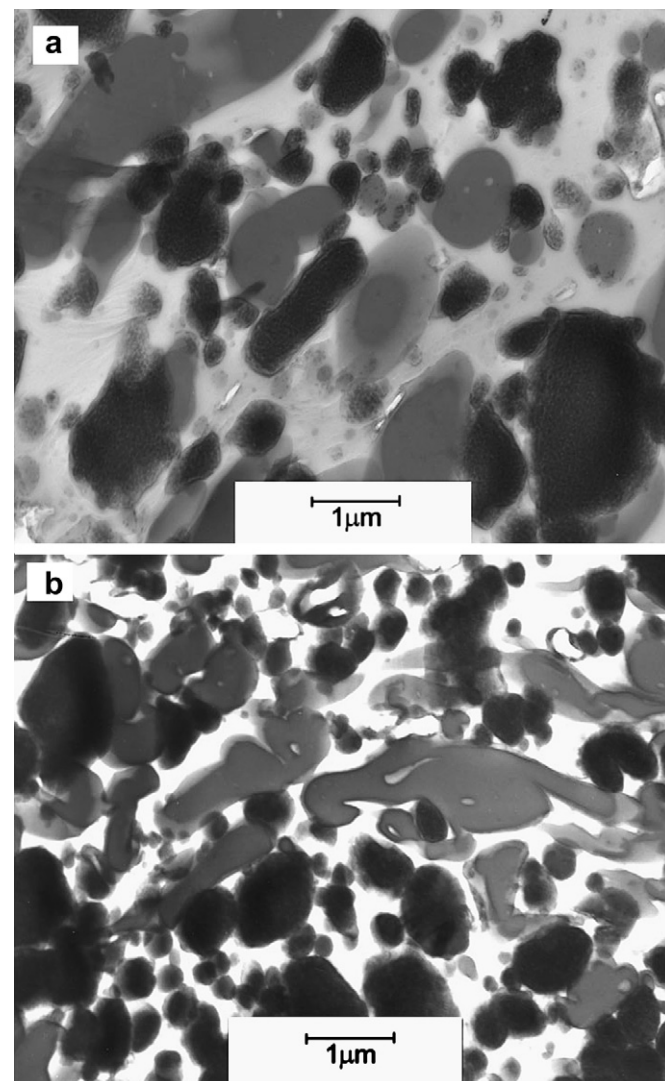


Fig. 5. TEM micrographs of 4 component blends. (a) PLA-I/PC/SEBS/EGMA = 60/20/15/5 (PPA-Zn, 3phr loaded), (b) PLA-I/PC/SEBS/EGMA = 40/40/15/5 (PPA-Zn, 3phr loaded).

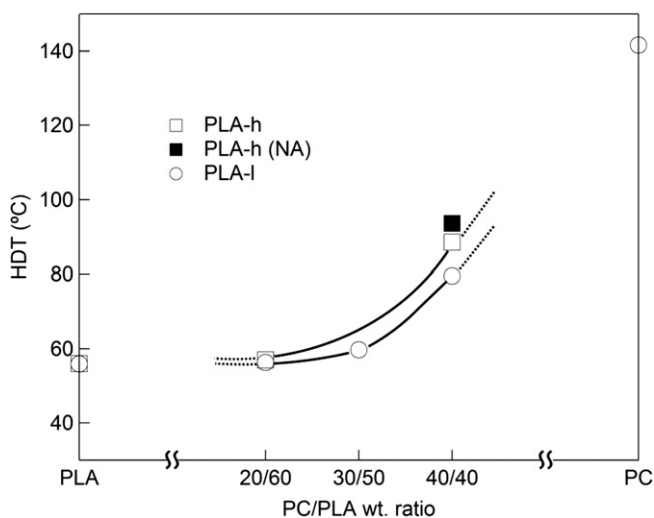


Fig. 4. Heat deflection temperature, HDT, as a function of PC content, as compared with neat PLA and PC. ■: nucleating agent PPA-Zn is loaded (3phr).

Fig. 2 shows Izod impact strength as a function of PC content. In Fig. 2a, the impact strength increases with increasing PC content. The aged systems have the lower impact strength than the as-mold ones. At PC/PLA = 40/40 composition, the difference is quite small, as compared with that of neat PC. Fig. 2b shows that the impact strength of as-mold PLA-h system at 40/40 wt. ratio is higher than that of corresponding PLA-l system (Fig. 2a). The high strength is maintained even for the aged system. That is, a super-tough alloy with excellent aging resistance is fabricated at PC/PLA-h = 40/40; i.e., PLA-h/PC/SEBS/PC = 40/40/15/5 (VIII).

Fig. 3 shows the tensile properties of PLA-h systems. Tensile moduli of the blends are slightly lower than that of neat PLA but almost same level as PC. It means that the stiffness is not sacrificed so much by blending the soft components, SEBS and EGMA. The modulus of aged samples is slightly higher than that of as-cast ones. It may be caused by the crystallization of PLA during the annealing. Elongation at break ( $E_b$ ) is much improved by the blending, as compared with neat PLA. At 40/40 composition, the  $E_b$  retention is fairly good; i.e., the ductile nature is not deteriorated so much by the annealing.  $E_b$  of the aged blends is same as neat PC, suggesting the nice performance as engineering plastics.

Fig. 4 shows the heat deflection temperature (HDT) as a function of PC content. As expected, HDT increases by increasing the high  $T_g$

component PC. To elevate the HDT further, we loaded 3 phr of a nucleating agent for PLA, zinc phenylphosphonate (PPA-Zn) for the samples IV, VI, and VIII. For IV and VI, the effect of PPA-Zn was negligibly small. Only for VIII, appreciable HDT elevation was observed as indicated by ■ in Fig. 4.

Figs. 5 and 6 show the TEM micrographs of samples IV (Fig. 5a), VI (Fig. 5b), VII (Fig. 6a), and VIII (Fig. 6b). Referring to Fig. 1, grey and dark regions are assigned to PC and SEBS particles, respectively. SEBS particles are not dispersed in PC particles but preferentially in PLA matrix. Compared with the PLA-l systems in Fig. 5, the PC particles in PLA-h system in Fig. 6 are highly elongated. The elongated PC particles render a somewhat bicontinuous nature that may provide the higher HDT than in the PLA-l systems (Fig. 5).

Fig. 7 shows the results of DMA in terms of the temperature dependence of the dynamic loss ( $\tan \delta$ ) of the sample VI, which exhibits the super-toughness and high HDT, and the component polymers; PLA, PC, and SEBS. In the sample VI,  $\tan \delta$  peak appears at  $T_g$  of neat PLA (around 70 °C). Another  $\tan \delta$  peak is seen near the peak temperature of neat SEBS (ca. -41 °C). But, it is definitely lower than that of neat SEBS. The difference, i.e.,  $T_g$  depression is 10 °C.

At lower temperature region, a broad  $\tan \delta$  peak is seen for neat PC. It is associated with the so-called  $\beta$ -relaxation temperature ( $T_\beta$ ) at which the local segmental motion start up. Similar peak is not obvious for PLA in Fig. 7 but it is clearly seen at a temperature indicated by arrow in Fig. 8 when the  $\tan \delta$  curve is highly magnified. In the sample VI,  $T_\beta$  peak appears at much lower temperature (around -22 °C) than PC. The difference is ca. 40 °C. It suggests that the local motion of PLA and PC chains in the blend can start up below  $T_\beta$  of neat PC. In other words, the local segmental motion in the blend VI should be highly active at room temperature (temperature for tensile and impact tests), compared with neat PC and PLA. Hence, the plastic matrix in the blend could be more ductile. Note that a PLA/PC = 50/50 blend without rubber component does not show such  $T_\beta$  depression as shown in Fig. 8.

Then, to be discussed is why the  $T_\beta$  is decreased by the presence of SEBS. The answer may be given by the  $T_g$  depression of EB (ethylene-co-butylene block of SEBS). The  $T_g$  depression has been observed in rubber toughened plastics, e.g., HIPS (high impact polystyrene) and ABS (acrylonitrile-butadiene-styrene copolymer) [19,20], the blend of styrene-butadiene-styrene block copolymer with corresponding homopolymers [21], aramid-butadiene

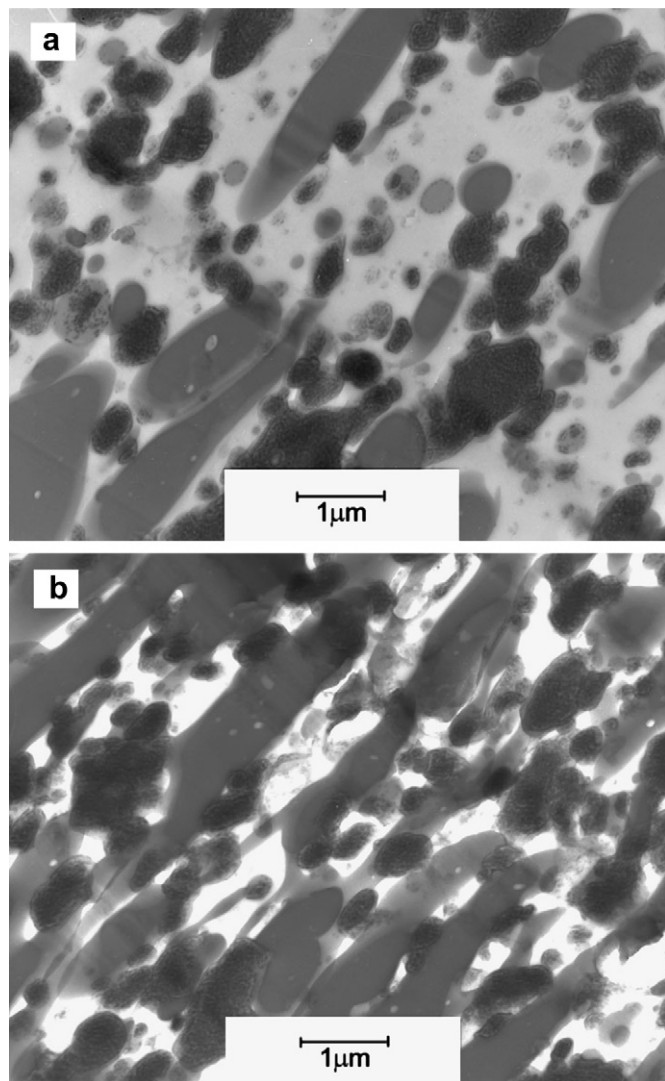


Fig. 6. TEM micrographs of 4 component blends. (a) PLA-h/PC/SEBS/EGMA = 60/20/15/5, (b) PLA-h/PC/SEBS/EGMA = 40/40/15/5 (PPA-Zn, 3phr loaded).

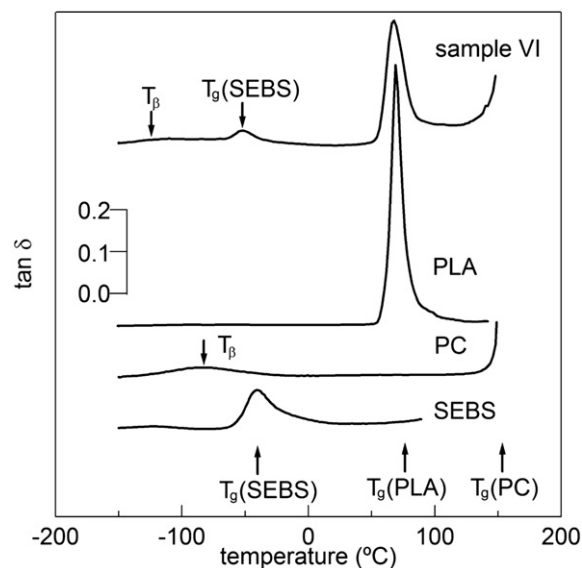


Fig. 7. Temperature dependence of the dynamic loss ( $\tan \delta$ ) of PLA/PC/SEBS/EGMA = 40/40/15/5 blend (sample VI) and the component polymers.

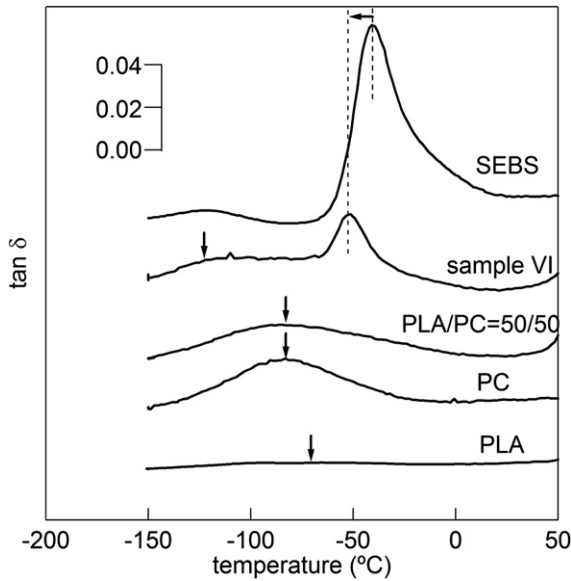


Fig. 8. Magnified figure of the low temperature region in Fig. 7. (A data of PLA/PC = 50/50 blend is added).

multiblock copolymer [22], and PBT alloy [17]. The  $T_g$  depression is explained by the negative pressure imposed on the dispersed rubber phase, resulting from differential contraction due to the thermal shrinkage mismatch upon cooling from liquid state. That is, after the material is cooled down below  $T_g$  of matrix, the rubber phase continues to shrink at the high shrinkage coefficient (thermal expansion coefficient of liquid state) in a closed space surrounded by the glassy polymer matrix which has a much lower shrinkage coefficient (of glassy state). The negative pressure in the dispersed rubber particles, in turn, would provide dilational stress fields for the matrix ligament between the particles. The dilational stress would lead to a loose segment–segment aggregation which may be favorable for the local segmental motions.

Both the  $T_g$  and  $T_\beta$  depressions were not affected by the annealing. As discussed above (concerning Fig. 1), the DSC analysis showed the crystallization of PLA by the annealing. The results in Fig. 2 imply that the negative pressure effect can be maintained

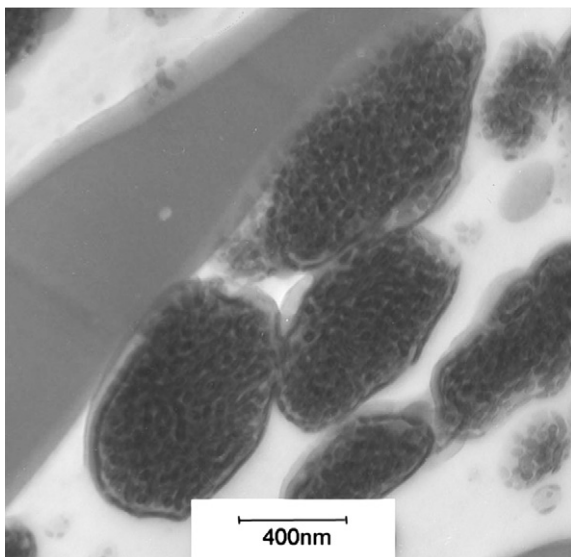


Fig. 9. TEM micrograph of PLA-h/PC/SEBS/EGMA = 60/20/15/5; magnified from Fig. 6a.

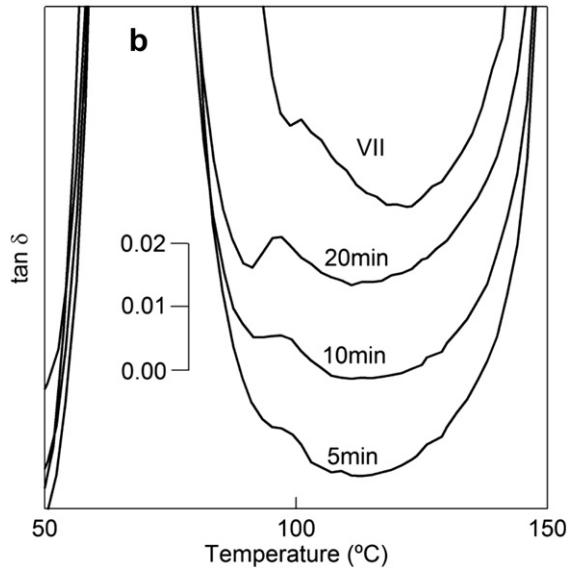
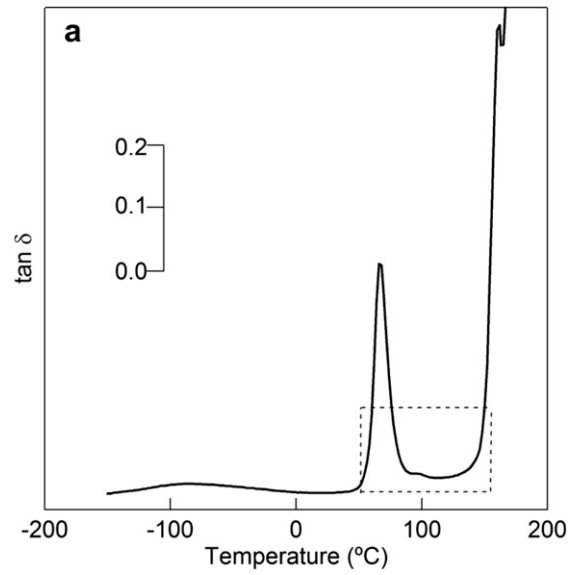


Fig. 10. (a) DMA data for PLA-I/PC = 50/50 blend melt-mixed at 240 °C for 10 min (b) Magnified curves between  $T_g$ 's of PLA and PC. Mixing time was varied. A curve of sample VII (magnified from Fig. 7) is also shown.

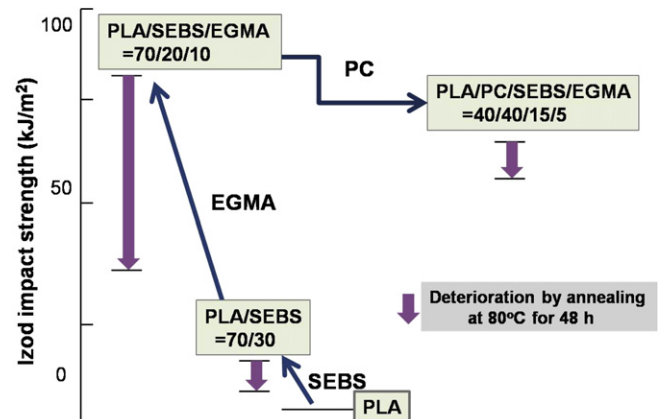


Fig. 11. Summarized stream for the development of super-tough 4 component alloy.

**Table 3**

Properties of PLA-h/PC/SEBS/EGMA-40/40/15/5 alloys injection-molded in cold (40 °C) and hot (80 °C) molds.

	40 °C molding		80 °C molding	
	as-mold	aged <sup>a</sup>	as-mold	aged <sup>a</sup>
Izod impact strength (kJ/m <sup>2</sup> )	65.9	61.7	63.3	59.2
Elongation at break (%)	86.1	59.2	91.7	84.7
Tensile modulus (GPa)	1.84	2.05	1.93	1.99
HDT (°C)	88.6		94.5	

<sup>a</sup> by annealing at 80 °C for 48 h.

even after the annealing and it makes the crystallized PLA ductile, leading to the toughened plastics.

To be further discussed is the adhesion between PLA and PC phases. As seen in TEM pictures in Figs. 5 and 6, SEBS particles are dispersed in PLA phase but not in PC phase. The dilational stress evolved in PLA phase by the negative pressure effect should be transferred to PC phase. Otherwise, the PC phase cannot be dilated. As shown in Fig. 2, neat PC deteriorates so seriously by the annealing that the PC phase in the blend may also become brittle. The embrittled PC phase could be toughened by the transfer of dilational stress.

Fig. 9 is a magnified TEM micrograph of Fig. 6a. Between the elongated PC particle and PLA matrix, a grey boundary is seen. The boundary may be assigned to a multiblock or random copolymer formed by the exchange reactions between PLA and PC during melt mixing. The copolymer is expected to enhance the interfacial adhesive strength. The formation of such copolymers is supported by DMA data in Fig. 10.

Fig. 10a shows the  $\tan \delta$  curve of a PLA/PC = 50/50 blend prepared by melt mixing at 240 °C for 10 min in a compact (100 ml) batch mixer with two brades, Laboplastomill, Toyo Seiki Co. Ltd. The batch mixer was used to prepare a series of samples with different mixing time. The  $\tan \delta$  curve between the  $T_g$  of PLA and  $T_g$  of PC is magnified and shown in Fig. 10b. A small  $\tan \delta$  peak appears near 100 °C and becomes bigger with increasing mixing time. Similar  $\tan \delta$  peak is seen also for the sample VII. The  $\tan \delta$  peaks should be assigned to the  $T_g$  of the copolymers formed by exchange reactions between PC and PLA.

#### 4. Conclusion

Thus, PLA was toughened by SEBS with the aid of reactive compatibilizer EGMA. The aging resistance and HDT were improved by incorporating PC. The stream of this development is briefly summarized in Fig. 11. Properties of the high performance PLA alloy are summarized in Table 3. Table 3 shows that the high performance is maintained after the annealing at high temperature and it does not depend on the molding temperature; i.e., the high temperature (80 °C) molding is not required for the PLA alloy. Note that all drawbacks of PLA have disappeared in the alloy. The outstanding ductile nature seems to come from the negative pressure effect of SEBS that dilates the PLA/PC matrix to enhance the local segment motions.

#### References

- [1] Karst D, Yang Y. *Polymer* 2006;47:4845–50.
- [2] Pezzin APT, Duek EAR. *J Appl Polym Sci* 2006;101:1899–912.
- [3] Machado AV, Moura I, Duarte FM, Botelho G, Nogueira R, Brito AG. *Int Polym Process* 2007;22:512–8.
- [4] Buchanan CM, Dorschel DD, Gardner RM, Komarek RJ, White AW. *J Macromol Sci Pure Appl Chem* 1995;32:683–97.
- [5] Negrin CM, Delgado A, Liabres M, Evora CJ. *Control Release* 2004;95:413–21.
- [6] Simon CG, Eidelman N, Kennedy SB, Sehgal A, Khatri CA, Washburn NR. *Biomaterials* 2005;26:6906–15.
- [7] Ronkko S, Rekonen P, Sihvola R, Kaarniranta K, Puustjarvi T, Terasvirta M, et al. *Biomed Mater Res. Part A* 2009;88:717–24.
- [8] Sun MZ, Downes SJ. *Mater Sci. Mater Med* 2009;20:1181–92.
- [9] Broz ME, VanderHart DL, Washburn NR. *Biomaterials* 2003;24:4181–90.
- [10] Semba T, Kitagawa K, Ishiaku US, Hamada HJ. *J Appl Polym Sci* 2006;101:1816–25.
- [11] Todo M, Park SD, Takayama T, Arakawa K. *Engng Fracture Mech* 2007;74:1872–83.
- [12] Ren J, Liu Z, Ren T. *Polym Polym Compos* 2007;15:633–8.
- [13] Harada M, Iida K, Okamoto K, Hayashi H, Hirano K. *Polym Eng Sci* 2008;48:1359–68.
- [14] Vilay V, Mariatti M, Ahmad Z, Pasomsouk K, Todo MJ. *J Appl Polym Sci* 2009;114:1784–92.
- [15] Vannaladsaysy V, Todo M, Takayama T, Jaafar M, Ahmad Z, Pasomsouk KJ. *Mater Sci* 2009;44:3006–9.
- [16] Zhang N, Wang Q, Ren J, Wang LJ. *Mater Sci* 2009;44:250–6.
- [17] Hashima K, Usui K, Fu L, Inoue T, Fujimoto K, Sagawa K, et al. *Polym Eng Sci* 2008;48:1207–13.
- [18] Wu S. *Polymer* 1985;26:1855–63.
- [19] Bohn L. *Angew Makromol Chem* 1971;20:129–40.
- [20] Morbitzer L, Ott KH, Schuster H, Kranz D. *Angew Makromol Chem* 1972;27:57–80.
- [21] Bates FS, Cohen RE, Argon AS. *Macromolecules* 1983;16:1108–14.
- [22] Inoue T, Ogata S, Kakimoto M, Imai Y. *Macromolecules* 1984;17:1417–9.